IJIREEICE

ISSN (Online) 2321 – 2004
ISSN (Print) 2321 – 5526

International Journal of Innovative Research in
Electrical, Electronics, Instrumentation and Control Engineering

ISO 3297:2007 Certified

Vol. 4, Issue 9, September 2016

Comparison of PI, Higher order and First order of Auto Disturbance Rejection Controller for Induction Motor Drives

G. Mounika[1], M. Nagaraju M.Tech [2]

M.Tech, PG Scholar, Department of EEE, Vignan`s Lara Institute of Technology &Science, Vadlamudi, Guntur, A.P[1]

Asst. Professor, Department of EEE, Vignan`s Lara Institute of Technology &Science, Vadlamudi, Guntur, A.P[2]

Abstract: A nonlinear auto disturbance rejection controller (ADRC) has been developed to ensure high dynamic performance of induction motors. Compared with the existing high-order ADRC-based speed control structures, the proposed method does not need to estimate the rotor flux. By using extended state observer (ESO), ADRC can accurately estimate the derivative signals and precise decoupling of induction motors is achieved. In addition, the proposed strategy realizes the disturbance compensation without accurate knowledge of induction motor parameters. The simulation and experimental results show that the proposed controller ensures good robustness and adaptability under modeling uncertainty and external disturbance. It is concluded that the proposed topology produces better dynamic performance, such as small overshoot and fast transient time, than the conventional proportional/integral (PI) controller in its overall operating conditions.

Keywords: Auto disturbance rejection controller, rotor flux, extended state observer

I. INTRODUCTION

Induction motors can be controlled similarly as dc motors using the field-oriented control (FOC) (also called vector control) approach, and the performances of the controlled induction motors with FOC are comparable to those of the dc motors. With the development of the power electronics elements and the high-performance microprocessor, induction motor drives employing FOC and conventional proportional–integral (PI) regulators have been commercialized. However, the performances of the PI regulator-based FOC suffers from the induction motor parameters' mismatch or variation with time in addition, when the load disturbances are present, the PI controller scheme has a long recovery period.

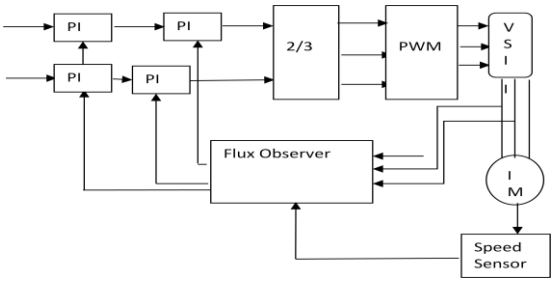

Fig.1. Control system of induction motor using PI controllers

This paper introduces a new configuration called auto-disturbance rejection controller (ADRC) into the control of induction motors. The ADRC was proposed by Han in 1998. The ADRC is a nonlinear controller for an uncertain system, it estimates and compensates the external disturbances and parameter variations, and as a consequence, the accurate model of the plant is not required. It means that the design of ADRC is inherently independent of the controlled system model and its parameters. The core of ADRC is the extended state observer (ESO), which is based on the concept of generalized derivatives and generalized functions. Using the extended state observer, the ADRC can realize accurate decoupling of induction motors. In addition, the impact of external disturbances and parameter variations could also be estimated and compensated by the ADRC.

Therefore, the accurate knowledge of the induction motor model is not required. As a result, the design of ADRC is inherently independent of the controlled system model and its parameters. Therefore, this controller has the advantage of good adaptability and robustness. This paper present the proposed controller can provide not only good speed regulation, but also excellent speed dynamic performance under large variations of drive system parameters and load conditions. Furthermore, the existing works usually use the second-order (or third-order) ADRCs, including the third-order (or fourth-order) dynamical equations for ESO. Consequently, the complexity of the entire control algorithm is dramatically increased. In this paper, a novel control scheme based on three first-order ADRCs is presented. The rotor flux estimation is removed to reduce the runtime of the proposed ADRC control algorithm. Because the order of ADRC is low and the flux estimation

IJIREEICE

ISSN (Online) 2321 – 2004
ISSN (Print) 2321 – 5526

International Journal of Innovative Research in
Electrical, Electronics, Instrumentation and Control Engineering

ISO 3297:2007 Certified

Vol. 4, Issue 9, September 2016

is removed the proposed simplified ADRC robust speed control scheme provides strong ability to resist the uncertainties, such as external load disturbances and Motor parameter variations.

II.MODEL OF INDUCTION MOTOR

Based on the reference-frame theory and the rotor flux orientation, the state space model of a squirrel case induction motor in a synchronous d-q reference frame can be described by fourth order nonlinear differential equation:

$$i_{d1} = -k_1 i_{d1} + k_2 \varphi_{d2} + i_{q1}\omega_1 + \frac{1}{\sigma} u_{d1} \quad (1\text{-}1)$$

$$\dot{\varphi}_{d2} = \frac{L_m}{T_r} i_{d1} - \frac{1}{T_r} \varphi_{d2} \quad (1\text{-}2)$$

$$\dot{\omega}_r = k_3 \varphi_{d2} i_{q1} - \frac{n_p}{J} T_L \quad (1\text{-}3)$$

$$i_{q1} = -k_1 i_{q1} - \frac{L_m}{\sigma L_r} \varphi_{d2}\omega_r - i_{d1}\omega_1 + \frac{1}{\sigma} u_{q1} \quad (1\text{-}4)$$

Where

$$T_r = \frac{L_r}{R_r} \qquad \sigma = L_s - \frac{L_m^2}{L_r}$$

$$k_1 = \frac{R_s L_r^2 + R_r L_m^2}{\sigma L_r^2} \qquad k_2 = \frac{R_r L_m}{\sigma L_r^2} \qquad k_3 = \frac{n_p^2 L_m}{J L_r}$$

u_{d1}, u_{q1}	d - Axis (q- axis) stator voltage
i_{d1}, i_{q1}	d - Axis (q - axis) stator current
$\varphi_{d2}, \varphi_{q2}$	d - Axis (q- axis) rotor flux
ω_1	Rotating speed of the coordinate
ω_r	Rotor angular speed
T_L	Load torque
R_s, R_r	Stator and rotor resistance s
L_s, L_r, L_m	Stator, rotor and mutual inductance s
J	rotor inertia
n_p	Pole pairs

Previous equations show that the mathematical model of the induction motor is affected by the following drawback

- The system is nonlinear due to the coupling parts between state variables .
- Motor parameters vary with operation condition.
- The load torque must be known.

III. CONTROL STRATEGY

A. Limitations of Conventional Vector Control in Speed Regulation of Inductor Motor

In the conventional FOC, PI regulators are used to control the flux magnitude, rotor speed, and currents independently (shown in Fig. 1), where represents the overall effect of external disturbances, parameter variations, and plant nonlinear dynamics. In PI controllers, the derivatives of the signals are required in order to achieve control objectives, such as reduced response time and reduced overshoot during transient conditions. Unfortunately, the derivatives of signals are difficult to retrieve because of noise. Furthermore, due to nonlinearities and uncertainties existing in the induction machine drive system, it is difficult for the conventional PI controller to achieve good static and dynamic performance for different operating situations. As a consequence of these phenomena, a degradation of drive performance occurs. To avoid these problems, a great deal of research has been done involving alternative control techniques.

In recent years, adaptive methods and predictive PI controllers have become more attractive in the improvement of the robustness and dynamic performance of control systems. However, they are very complex and require knowledge of model parameters and model states. As a consequence, they require high computational intensity in real-time implementation. One effective way to design a controller is to get rid of the restriction of the mathematical model.

This would promote a new structure of controllers. Based on the theory of nonlinear feedback and generalized derivatives, ADRC is introduced in this paper. For the FOC scheme of induction motors, three control loops, including the quadrature axis (q-axis) current loop, the direct axis (d-axis) current loop, and the speed loop, are considered. Fig. 1(a) shows an example of the induction motor speed control system using high-order ADRCs, which consists of two second-order ADRCs for the speed control and q-axis current control, respectively, and one third-order ADRC for the d-axis current control. Meanwhile, the flux estimator is needed to get the information about flux and rotor angle. Fig. 1(b) gives the proposed scheme using three first-order ADRCs for the speed control of induction motors, where three first-order ADRCs are used for the three control loops of the system. It is shown from Fig. 1 that the proposed control scheme is simpler in the sense of using lower order ADRCs, which means the lower order of dynamical equation to be solved and that the removal of the flux estimator further reduces the complexity of the control algorithm.

B. Advantages of Nonlinear Feedback Compared With Linear Feedback

In many respects, a nonlinear system has some high efficient characteristics compared to a linear system. To give a simple example, consider the system $\dot{x} = \omega(t) + u(t)$, where $\omega(t)$ is the disturbance and the u(t) control signal is designed to stabilize the whole system. Using the linear feedback $u = -kx$ control ,at the steady-state $\dot{x} = 0$, the steady-state error of the closed loop is $e = \omega(t)/k$(assuming k> $\omega(t)$). By choosing nonlinear feedback control $u = -kx^{\propto}$ sign(x),0<$\propto$<1, where sign(x) is the signum function. The magnitude of steady-state error is reduced to $|e| = |w(t)/k|^{\frac{1}{\alpha}} < |w(t)/k|$ .This indicates that a proper nonlinear feedback control can significantly reduce the effect of disturbance compared with linear feedback.

IJIREEICE

ISSN (Online) 2321 – 2004
ISSN (Print) 2321 – 5526

International Journal of Innovative Research in
Electrical, Electronics, Instrumentation and Control Engineering

ISO 3297:2007 Certified

Vol. 4, Issue 9, September 2016

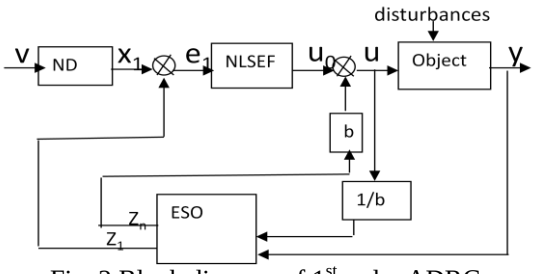

Fig. 2 Block diagram of 1st order ADRC.

C. Auto disturbance rejection controller

Based on the nonlinear feedback, the nonlinear auto-disturbance rejection controller (ADRC) is introduced to achieve high dynamic performance in the overall operating range. It is composed of three parts (shown in Fig. 2): 1) nonlinear differentiator (ND), 2) extended state observer (ESO), and 3) nonlinear state error feedback control law (NLSEF). The essential part of ADRC is the extended state observer. The ESO in the ADRC can be treated as a kind of dynamic feedback linearization mechanism. Its structure and performance are not only determined by the model of the system under control, but only by the range of its variation rate. Therefore, the ESO is robust to the system model uncertainty. The role of ND is to define a desirable transition response for the step input. The ND can smoothen the sudden change of the input signal in order to decrease the overshoot of the output response during the transient state. These factors make ADRC get a good balance between the fast transient response and the small overshoot. On the contrary, for the conventional PI controller, it is hard for tuning parameters to achieve this point. The NLSEF gives the control law u0 to drive the state trajectory to track the desired reference.

1) Structure of Extended State Observer (ESO):

Based on the theory of generalized derivative and generalized functions, ESO is a nonlinear configuration for observing the states and disturbances of the system under control without the knowledge of the exact system parameters. Giving an example, for any arbitrary Nth order nonlinear system

$$x^{(n)} = f(x, \dot{x}, \dots \dots x^{(n-1)}, t) + \omega(t) + c \cdot u(t) \quad (2)$$

where f(t) represents the arbitrary system function, ω(t) is an unknown disturbance, u(t) is the control law, x(t) is the measurable state variable, and c is the coefficient of control law. Its state space equation can be written as

$$\begin{aligned} \dot{x}_1 &= x_2 \\ &\vdots \\ \dot{x}_{n-1} &= x_n \end{aligned}$$

$$\dot{x}_n = f(x, \dot{x} \dots, x^{(n-1)}, t) + \omega(t) + cu \quad (3)$$

where $x_1 = x, x_2 = \dot{x}, \dots, x_n = x^{(n-1)}$, .

Unlike the full order (N th order) state observer, ESO utilizes (N+1)th order (full order plus 1) state observation to achieve state and disturbance estimation [shown in (3)]. After startup, the output of the ESO $z_1, \dots, z_n$ will converge quickly and accurately to the observed states $x_1, x_2, \dots, x_n$. The initial values of $z_1, \dots, z_n . z_{n+1}$ are all set to be zero

$$\begin{aligned} \dot{z}_1 &= z_2 - g_1(z_1 - x_1(t)) \\ &\vdots \\ \dot{z}_n &= z_{n+1} - g_n(z_1 - x_1(t)) + c \cdot u(t) \\ \dot{z}_{n+1} &= -g_{n+1}(z_1 - x_1(t)) \\ g_i(z_1 - x_1(t)) &= \beta_i \text{fal}(z_1 - x_1(t), \alpha, \delta) \end{aligned}$$

i=1,….,n+1

$$\text{fal}(\varepsilon . \alpha_i, \delta) = \begin{cases} |\varepsilon|^{\alpha} \text{sgn}(\varepsilon), & |\varepsilon| > \delta \\ \frac{\varepsilon}{\delta^{1-\alpha}} & |\varepsilon| \le \delta \end{cases} \quad (4)$$

where $= z_1 - x_1(t)$, sign(ε) is the signum function. The exponential $\alpha \in (0,1)$is usually set to be$\alpha = (m/2^n)(n = 1,2,\dots,$and $m \le 2n.\alpha$ and the scaling factor βideterminethe convergence speed of ESO. The parameter δdetermines the nonlinear region of the ESO.

Nonlinear state feedback in the ESO is used to achieve linearization of nonlinear systems [shown in (3)]. As mentioned previously, the derivative signals are often difficult to obtain because of noises. But in the ESO, lower order derivatives (such as $z_1(t), \dots, z_n(t)$) are obtained by integrating the higher order derivatives $z_2(t), \dots, z_{n+1}(t)$. The differential operation is no longer needed. As a result, the differential signal is noise free. The generalized derivatives of given signals will be accurately achieved.

Furthermore, if we define $x_{n+1}(t) = f(x, \dot{x}, .., x^{(n-1)}, t + \omega t,$ where fx,x,…,x(n−1),t represents the system modeling uncertainty and ω(t) represents the unknown disturbance, then (2) can be rewritten as

$$\begin{aligned} \dot{x}_1 &= x_2 \\ &\vdots \\ \dot{x}_n(t) &= x_{n+1}(t) + c.u(t) \\ \dot{x}_{n+1}(t) &= b(t) \end{aligned} \quad (5)$$

where b(t) is the variation rate of system uncertainty and disturbance $x_{n+1}(t)$

Subtracting (5) from (4), the dynamic error equation is defined as

$$\begin{aligned} \delta\dot{x}_1 &= \delta x_2 - g_1(\delta x_1) \\ &\vdots \\ \delta\dot{x}_n &= \delta x_{n+1} - g_n(\delta x_1) \\ \delta\dot{x}_{n+1} &= -b(t) - g_{n+1}(\delta x_1) \end{aligned} \quad (6)$$

IJIREEICE

ISSN (Online) 2321 – 2004
ISSN (Print) 2321 – 5526

International Journal of Innovative Research in
Electrical, Electronics, Instrumentation and Control Engineering

ISO 3297:2007 Certified

Vol. 4, Issue 9, September 2016

Where δx_1 is $z_i - x_i$ and i is 1,….,n+1 .
For any boundary b(t), when the nonlinear functions $g_i(z)$ and their related parameters α, β_i and δ are properly selected to constrain the function of system uncertainties and disturbances, the system (6) is asymptotic stable. Under this condition, the state variables of ESO,$z_i(t)$, i=1,….,n, will quickly converge to the observed state variables x(t) and its derivatives $\dot{x(t)}, \ddot{x(t)}, \ldots, x^{n-1}(t)$. Furthermore, the signal of (N+1) th state variable $z_{n+1}(t)$ reveals the information about the overall impact of external disturbances and plant uncertainties imposed on the system under control. Based on this information, compensation and elimination of disturbances and model uncertainties can be achieved. If the variation rate b(t) has some boundary, the overall effect of the external and internal disturbances $x_{n+1}(t)$ imposed on the system can be observed by $z_{n+1}(t)$successfully, even though the mathematic expression and accurate parameters of f(t) and $\omega(t)$ may be still unknown. It will greatly enhance the robustness of the control system against the modeling uncertainties and disturbances.
By using the ESO, the whole nonlinear system is decomposed into integrators in cascade, so the feedback linearization is realized. Similar to input-output feedback linearization, the ESO can be treated as some kind of dynamic feedback linearization. However, its architecture and performance are not determined by the actual expression of system under control, but only affected by the range of its variation rate. Therefore, this observer has good robustness and adaptability. This is the main advantage of this configuration.

2) Structure of Nonlinear Differentiator (ND):
The second part of ADRC is a th order nonlinear differentiator. The objective of ND is to define a desirable transition response when the input changes. Its input is the reference signal v(t), the output of ND is the pre modulated reference signal $\mathbf{z_1(t)}$and its derivative $\mathbf{z_1(t)}, \ldots, \mathbf{z_n(t)}$ (as shown in Fig. 2).

The mathematic model of nonlinear differentiator is given as (6), shown at the bottom of the next page, where v(t)is the given input reference signal,$z_1(t)$ is the pre modulated signal of v(t), are the modulated first to(N-1) th order derivatives of v(t) ,sgn(ε) and is the signum function. r is the scaling factor of ND. It influences the converge speed of ND. $b_1, \ldots, b_{n-1}$ Is the fine tuning factors of ND. and serve the same function as that in ESO.

In the conventional PI controller, it is hard to achieve fast response and reduced overshoot at the same time. This is because the PI controller utilizes the original given signals directly. Any sharp change (step change) in the given signal could lead to overshoot in the output. In the th order nonlinear differentiator, the given input signal v(t) is regulated to a continuous smooth curve $z_1(t)$, whose derivatives $z_1(t), \ldots, z_{n-1}(t)$ are also continuous, smooth, and finite. That means ND can smooth the sharp changes in the input signal, so that the ADRC could still maintain no overshoot during the fast transient process, even though the input signal may change suddenly.

It can be seen from (6), that the mathematical function of the nonlinear differentiator is a nonlinear structure with linear intervals near the original point. The merit of this topology is that it can fully utilize the nonlinear characteristics for large signals. At the same time, the phenomenon of chatting near the origin is avoided. In the linear intervals, the nonlinear

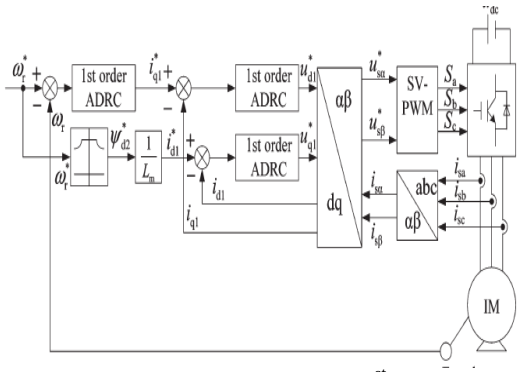

Fig 3a Control system using three 1st order ADRC

Differentiator acts as a very good low pass filter. Similar to ESO, lower order derivatives [such as $z_1(t), \ldots\ldots, z_{n-1}(t)$] are also achieved by integrating the higher order derivatives $z_2(t), \ldots., z_n(t)$. The contained noises are all constrained, not enlarged, so that ND can get high quality derivatives as well.

3) Structure of Nonlinear State Error Feedback Control Law (NLSEF):
As shown in Fig. 2, the nonlinear differentiator generates the arranged transition process and its derivatives $z_{11}, \ldots., z_{1n}$. The outputs of extended state observer $z_{21}, \ldots. z_{2n}$ estimate the states of a controlled system. By comparing the difference between the outputs of nonlinear differentiator and those of extended state observer (shown in Fig. 2), the nonlinear state error feedback control law $u_0(t)$ is used to drive the state trajectory to the desired reference signal. Its mathematic expression is given as

$$u_0 = k_1 fal(\varepsilon_1, \alpha, \delta) + \cdots + k_n fal(\varepsilon_n, \alpha, \delta)$$

$$fal(\alpha.\varepsilon_i, \delta) = \begin{cases} |\varepsilon_i|^{\alpha} sgn(\varepsilon_i), & |\epsilon_i| > \delta \\ \frac{\varepsilon_i}{\delta^{1-\alpha}} & |\varepsilon_i| \le \delta \end{cases}$$

i=1,….,n (7)

where $\varepsilon_1 = z_{11} - z_{21}, \varepsilon_2 = z_{12} - z_{22}, \ldots., \varepsilon_n = z_{1n} - z_{2n}. k_i (i = 1, \ldots., n)$ is the scaling factor of NLSEF. and are the variable parameters of NLSEF and they serve the same function as that in ESO and ND. It can be seen from (7), that the nonlinear feedback structure is adopted. In

IJIREEICE

ISSN (Online) 2321 – 2004
ISSN (Print) 2321 – 5526

International Journal of Innovative Research in
Electrical, Electronics, Instrumentation and Control Engineering

ISO 3297:2007 Certified

Vol. 4, Issue 9, September 2016

addition, this configuration is independent of the object model. Furthermore, with the help of modeling uncertainty and disturbance estimation $z_{2,n+1}(t)$, online compensation is made by $u(t) = u_0(t) - z_{2,n+1}(t)/c$ [where c is the coefficient of control law in (1)]. The robustness of the system is guaranteed.

4) Advantages of ADRC:
From the previous sections, it can be seen that ADRC has many advantages.
a) The generalized derivatives of given signals can be obtained accurately.
b) With the help of nonlinear differentiator, ADRC could maintain no overshoot during the fast transient process, even though the input signal may change suddenly.
c) By using ESO, the whole nonlinear system is decomposed into integrators in cascade. Decoupling and dynamic feedback linearization are realized.
d) ADRC utilizes the online estimation and compensation to eliminate the steady-state error between input and output. Therefore, integrators are no longer needed. The desired behaviors of the control system such as tracking, regulation, and stability are guaranteed.
e) With the help of ESO and NLSEF, the system uncertainties and external disturbance could be estimated and compensated instantaneously and accurately. The control system's robustness is guaranteed.
f) The architecture and performance of all parts of ADRC are not determined by the actual mathematic model of the system under control, but only affected by the range of its variation rate. Therefore, ADRC has robustness and adaptability against the external disturbance, variation of system parameters, and model changes.

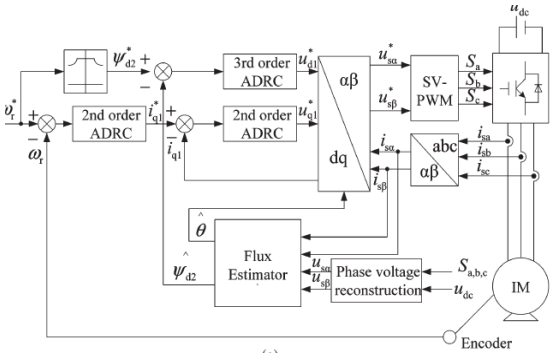

Fig. 3b Control system of induction motor using ADRC

In this paper, auto-disturbance rejection controllers (ADRC) are introduced to substitute the function of PI controllers to achieve high dynamic performance in the overall operating conditions (as shown in Fig. 3). As compared to the conventional PI scheme (as shown in Fig. 1), the control system includes two separate control loops: 1) the flux loop which uses one third-order ADRC to control the rotor flux and 2) the speed loop, which uses two second-order ADRC in cascade to control the rotor speed , and -axis stator current , respectively. These controllers are robust against load and parameter disturbances. In addition, precise decoupling and linearization of induction motor is realized by using ADRC. Good torque/speed response can be maintained without precisely knowing the position and magnitude of rotor flux.

Therefore, similar to direct torque control (DTC), the accurate flux observation in the control system is not required. This is one of the major advantages using ADRC into induction motor control.
In this section, the application of ADRC into flux control loop is discussed in detail. By differentiating (1-2), and combining with (1-1), the second-order derivative of flux is derived as

$$\ddot{\varphi}_{d2} = -\frac{1}{T_r}\dot{\varphi}_{d2} + \frac{L_m}{T_r}k_2\varphi_{d2} + \frac{L_m}{T_r}\left(-k_1 i_{d1} + i_{q1}\omega_1\right) + \frac{L_m}{T_r\sigma}u_{d1} \qquad (8)$$

As reported in (8), the third term $\frac{L_m}{T_r}\left(-k_1 i_{d1} + i_{q1}\omega_1\right)$ contains the information about the rotor speed, d-axis and q –axis current. In this term, the product of rotor speed and q-axis current $\frac{L_m}{T_r}\left(i_{q1}\omega_1\right)$ is the coupled part between flux loop and speed loop.

This coupled part would deteriorate the control performance. If the whole third term $\frac{L_m}{T_r}\left(-k_1 i_{d1} + i_{q1}\omega_1\right)$ (including the coupled part $\frac{L_m}{T_r}\left(i_{q1}\omega_1\right)$ is regarded as the modeling uncertainty or internal disturbance of system, the following substitution is made:

$$\ddot{\varphi}_{d2} = -\frac{1}{T_r}\dot{\varphi}_{d2} + \frac{L_m}{T_r}k_2\varphi_{d2} + (\omega_{11}) + \frac{L_m}{T_r\sigma}u_{d1} \qquad (9)$$

where $\omega_{11} = \frac{L_m}{T_r}\left(-k_1 i_{d1} + i_{q1}\omega_1\right)$ Equation (9) shows that the flux loop could be considered as a second-order subsystem. To control the rotor flux, a third-order ADRC is used. It is composed of three parts: 1) second-order nonlinear differentiator (ND), 2) third-order extended state observer (ESO), and 3) nonlinear state error feedback control law (NLSEF) (as shown in Fig. 4). Here, $\omega_1(t)$ represents the disturbances imposed on the flux subsystem. Their configurations are given in detail to illustrate how ADRC is used for induction motor control.

A. Second-Order ND for Flux Control
The flux loop is considered as a second-order subsystem, so second-order ND is used in the flux control loop (as shown in Fig. 4). It will arrange the flux transition process according to the input reference flux and the system under control. Its mathematic model is given as

$$\dot{z}_{11} = z_{12}$$
$$\dot{z}_{12} = -r.\left(\mathrm{fal}(z_{11} - \varphi_{d2}^{*}, \alpha, \delta) + b_1 \cdot \mathrm{fal}(z_{12}, \alpha, \delta)\right) \qquad (10)$$

IJIREEICE

ISSN (Online) 2321 – 2004
ISSN (Print) 2321 – 5526

International Journal of Innovative Research in
Electrical, Electronics, Instrumentation and Control Engineering

ISO 3297:2007 Certified

Vol. 4, Issue 9, September 2016

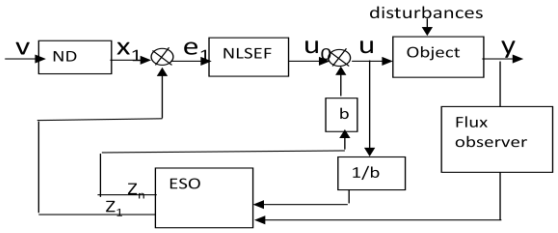

Fig. 4 Block diagram of third-order ADRC used in the flux control loop.

Where φ_{d2}^{*} the given reference is signal of rotor flux, $z_{11} = \hat{\varphi}_{d2}^{*}$ and $z_{12} = \hat{\varphi}_{d2}^{*}$ are the arranged flux transition process and its derivative (shown in Fig. 4). Parameters $r, \alpha, \delta, b1$, and function $fal(\varepsilon, \alpha, \delta)$ are defined in Section II-C2.

B. Third-Order ESO for Flux Control

In the flux control loop, a third-order ESO is utilized to achieve state and disturbance estimation (shown in Fig. 4). Its mathematic model is derived as

$$\begin{aligned} \dot{z}_{21} &= z_{22} - g_1(z_{21} - \hat{\varphi}_{d2}) \\ \dot{z}_{22} &= z_{23} - g_2\left((z_{21} - \hat{\varphi}_{d2}) + \frac{L_m}{T_r\sigma}u_{d1}\right) \\ \dot{z}_{23} &= -g_3(z_{21} - \hat{\varphi}_{d2}) \end{aligned} \quad (11)$$

Where $g_1(z_{21} - \hat{\varphi}_{d2}) = \beta_i fal(z_{21} - \hat{\varphi}_{d2}, \alpha, \delta)$, i=1,2,3.$\hat{\varphi}_{d2}$ is the observed flux by using flux observer and it is the input of ESO.$z_{21} = \varphi_{d2}^{'}$ and $z_{22} = \dot{\varphi}_{d2}^{'}$ and are the estimated rotor flux and its derivative by using ESO (shown in Fig. 4). The third-order state of ESO z_{23} reveals the overall influence of modeling uncertainty $\omega_{11}(t)$. The definition of parameters β_i, α, δ and function $fal(\varepsilon, \alpha, \delta)$ are all given in Section II-C1.

C. NLSEF for Flux Control

The NLSEF used in the flux control loop is to drive the rotor flux to the given reference flux. Its mathematical model is given as

$$u_{d0}(t) = k_1 fal(\varepsilon_1, \alpha, \delta) + k_2 fal(\varepsilon_2, \alpha, \delta) \quad (12)$$

$$u_{d1}(t) = u_{d0}(t) - c_1(t) \quad (13)$$

Where $\varepsilon_1 = z_{11} - z_{21} = \hat{\varphi}_{d2}^{*} - \varphi_{d2}^{'}, \varepsilon_2 = z_{12} - z_{22} = \hat{\varphi}_{d2}^{*} - \varphi_{d2}^{'}, u(t) = u_0(t) - \alpha(t)$, and z_{23} is the third-order state of ESO. The parameters k_1, k_2, α, δ , and function $fal(\varepsilon, \alpha, \delta)$ are defined in Section II-C3.

Similarly, when ADRC is applied to the speed control loop, the external load and the coupling part between the speed loop and flux loop can also be treated as internal disturbance. Therefore, (1-3) and (1-4) can be rewritten as

$$\dot{\omega}_r = k_3\varphi_{d2}i_{q1} + \omega_{21}(t)$$

$$\dot{i}_{q1} = -k_1 i_{q1} + \omega_{31}(t) + \frac{1}{\sigma}u_{q1} \quad (14)$$

Where $\omega_{21}(t) = -\frac{T_l n_p}{J}$represents the external load torque imposed on the system, and $\omega_{31}(t) = -\left({L_m}/{\sigma L_2}\right)\varphi_{d2}\omega_r - i_{d1}\omega_1$ is the coupled part between the flux and speed control subsystem.

In the speed subsystem, as shown in (14), the configuration of its control system is composed of two second-order ADRCs. One is used for speed regulation and another is used for –axis current control (shown in Fig. 3). Their structure and mathematical model are all similar to that of flux subsystem. Here, two second-order ESOs are used to estimate the rotor speed, q-axis current, and their derivatives. The model uncertainties $\omega_{21}(t)$and $\omega_{31}(t)$ are observed by the second-order states of ESO $z_{22-\omega}$ and z_{22-s} separately.

According to the theory of ADRC [6], because the variation ranges of $\omega_{11}(t), \omega_{21}(t)$ and $\omega_{31}(t)$ are finite, the external load disturbance and the coupled parts between the flux loop and speed loop can be completely estimated and compensated by ESO and NLSEF. Therefore, the dynamic equations of the whole system are simplified as

$$\begin{aligned} \ddot{\varphi}_{d2} &= -\frac{1}{T_r}\dot{\varphi}_{d2} + \frac{L_m}{T_r}k_2\varphi_{d2} + \frac{L_m}{T_r\sigma}u_{d0} \\ \dot{\omega}_r &= k_3\varphi_{d2}I_{q0} \\ i_{q1} &= -k_1 i_{q1} + \frac{1}{\sigma}u_{q0} \end{aligned} \quad (15)$$

where , , and are the control signals before compensation, and the given control signals after compensation can be defined as

$$u_{d1} = u_{d0} - \frac{z_{23}(t)}{\frac{L_m}{T_r\sigma}} \quad (16)$$

$$I_{q1} = I_{q0}\frac{-z_{22\_\omega}(t)}{k_3\varphi_{d2}} \quad (17)$$

$$u_{q1} = u_{q0} - z_{22\_s}(t)\cdot\sigma \quad (18)$$

Here $\frac{z_{23}(t)}{\frac{L_m}{T_r\sigma}}$, $\frac{-z_{22\_\omega}(t)}{k_3\varphi_{d2}}$, and $z_{22\_s}(t)\cdot\sigma$ are considered to be correction or compensation items. They are estimated by ESO, and then compensated by NLSEF separately.

It can be seen that due to the compensation made by NLSEF [shown in (16)–(18)], the whole system of the induction motor is simplified as (15). There is no coupled part between the flux control subsystem and speed control subsystem. The impact of external load disturbances is also eliminated.

Therefore, the decoupling of the rotor flux and speed control loop is achieved. Furthermore, this dynamic feedback linearization method doesn't need the actual

IJIREEICE

ISSN (Online) 2321 – 2004
ISSN (Print) 2321 – 5526

International Journal of Innovative Research in
Electrical, Electronics, Instrumentation and Control Engineering

ISO 3297:2007 Certified

Vol. 4, Issue 9, September 2016

expression of the mathematical model of induction motors. The robustness and adaptability of the control system is significantly improved.

As it is mentioned above, the dynamic model of the induction motor is precisely decoupled into two linear subsystems: 1) flux subsystem and 2) speed subsystem (shown in Fig. 5). It is obvious from Fig. 5, that the precise decoupling of flux/speed control and exact linearization can be achieved if ESO achieves the state and model disturbance estimation accurately. So, it is convenient to use a third-order ADRC to give out the flux control signal $u_{d1,}$ and use two second-order ADRC in cascade to send out the speed and current control signal i_{q1} and u_{q1} separately [9] (shown in Fig. 3).

It is observed, that rotor resistor and load torque changes most frequently when the induction motor is operating. For the ADRC presented in this paper, only the variation of rotor resistance and load torque are considered. Nevertheless, ADRC can also be used to compensate the variation of other parameters. Then, (9) (14) can be rewritten

$$\ddot{\varphi}_{d2} = -\frac{1}{T_r}\dot{\varphi}_{d2} + \frac{L_m}{T_r}k_2\varphi_{d2} + \omega_{11}(t) + \frac{L_m}{T_r\sigma}u_{d1} + \omega_{12}(t) \quad (19)$$

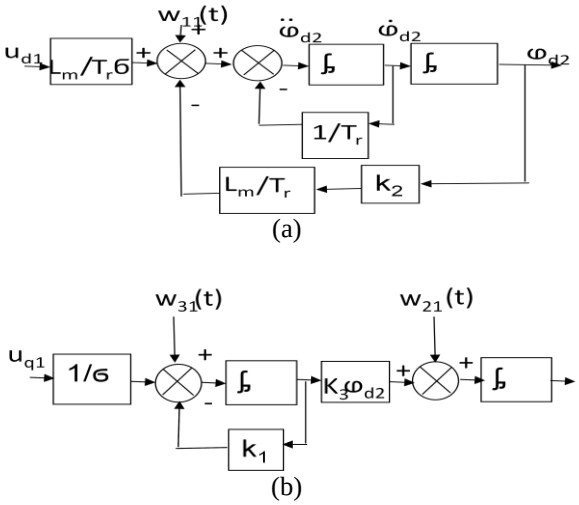

Fig. 5. Equivalent dynamic mathematical model of induction motor (a) flux subsystem and (b) speed subsystem.

$$\omega_{12}(t) = \left(\frac{1}{T_r} - \frac{1}{T_r}\right)\dot{\varphi}_{d2} + \left(\frac{L_m}{T_r}k_2 - \frac{L_m}{T_r}k_2\right)\varphi_{d2} + \left(\frac{L_m}{T_r\sigma} - \frac{L_m}{T_r\sigma}\right)u_{d1}$$

$$\dot{\omega}_r = k_3\varphi_{d2}i_{q1} + \omega_{21}(t) + \omega_{22}(t)$$

$$i_{q1} = -k_1 i_{q1} + \omega_{31}(t) + \frac{1}{\sigma}u_{q1} + \omega_{32}(t) \quad (20)$$

Where $\omega_{22}(t) = \Delta T_l \cdot \frac{n_p}{J}, \omega_{32}(t) = (k_1 - k_1') \cdot i_{q1}$, , and T_r', k_1' and k_2', are the induction motor coefficients when rotor resistant is changed . ΔT_l is the load torque change.

Based on (19) and (20), the external load change and internal parameter variation are all treated as disturbances imposed on the controlled system. Due to the fact that the variation range of load and parameter change is finite, then by properly selecting the functions and related parameters of ESO and NLSEF, we can accurately estimate and compensate the overall influence of parameter variation and external disturbance. These functions and parameters of ADRC are all independent of the object under control.

Therefore, the closed loop motor drive system under ADRC control does not depend on the accurate mathematical model of induction motors. It has good robustness and adaptability to parameter variation and load disturbance. This is the chief reason why ADRC is utilized here.

In Appendix B, the function of the ADRC parameters are analyzed and the method to adjust the parameters of ADRC is given. In Appendix C, all the values of ADRC parameters for the induction motor control used in this paper are listed.

IV. SIMULATION RESULTS

To show the performance of the proposed control scheme, an MATLAB/Simulink model has been established for a 1.1-kW induction machine driven by a voltage source inverter (VSI) using the proposed scheme. Each first-order ADRC is written by an S-function with C code. The parameters of the squirrel-cage induction motor are listed as follows:

PN =1.1 kW
UN =380 V
IN =2.67 A
fN =50 Hz
R1 =5.27 Ω
R2 =5.07 Ω
RFe =1370 Ω
L1 =479 mH
L2 =479 mH
Lm =421 mH
σ =0.228
TN =7.45 N · m
P =2
n_N =1410 r/min.

We have investigated the robustness of the proposed scheme under the following three cases a) load disturbance; b) the motor parameter variations; and c)the model uncertainty.

The proposed method is compared with the vector control based on the traditional PI regulators. In the simulation, both the adjustable parameters of the ADRC and those of the PI system have been manually tuned to their desirable values. It can be also done by the method proposed.

DOI 10.17148/IJIREEICE.2016.4903

IJIREEICE

ISSN (Online) 2321 – 2004
ISSN (Print) 2321 – 5526

International Journal of Innovative Research in
Electrical, Electronics, Instrumentation and Control Engineering

ISO 3297:2007 Certified

Vol. 4, Issue 9, September 2016

A. Load Disturbance Performance

In the steady-state performance aspect, the ADRC system can always settle down to the speed reference value without steady-state error, whereas the steady-state error of the PI system increases when the load is heavier, even up to 1.3% under rated load. This shows that the ADRC system has better robustness compared with the PI System from the viewpoint of load disturbances. In the dynamic performance aspect, the ADRC system always has larger overshoot than the PI system in the simulation results, the reason is that their linearization mechanisms are essentially different: the PI regulator depends on the field oriented to realize the decoupling of the torque control and the flux control, when the rotor flux direction coincides with the d-axis, under this circumstance, the induction motor can be treated as a "linear" system. However, in ADRC control scheme, the ESO, a core component of ADRC, estimate the internal and the external disturbances as the "total disturbance" in real time, then compensate it. As a result, the system is dynamically linearized. In a simulation model, the PI system uses the exact parameters, which means that the parameters used in the vector control scheme match very well with the motor; thus, the dynamic performance could be perfect if the parameters of the PI regulators are optimized. On the contrary, the dynamic performance of the ADRC depends on the dynamic performance of its ESO, when the load suddenly increases or decreases, the disturbances in (1), (5), and (6) of the three ADRCs will also suddenly change, the ESOs will undergo a transient state to estimate the disturbance and to track reference. Therefore, even if the ADRC parameters are good, the simulation results will inevitably overshoot when load torque steps up or down heavily in high speed range.

B. Parameter Variation Performance

To evaluate the rapidity and the accuracy of control algorithms, the step response of reference variation or the step response of disturbance is usually observed, because the step signal contains the most abundant frequency components. For induction motor drive systems, if wound-rotor induction motors were selected, the rotor resistance may suddenly increase or decrease. Although, the rapid parameter variation is not the general case, the step variation of the rotor resistance is still chosen here to do the comparative simulation, in order to evaluate the proposed ADRC scheme under the worst operation condition. A simulation motor model with a varying rotor resistance is used to simulate the performance of the proposed scheme

C. Model Uncertainty Performance

The speed reference steps up from 0.4 to 0.8 pu at 5 s, and the load torque is full load throughout the simulation. The motor parameters, including the iron loss equivalent resistance, are set as the parameters listed aforementioned. If the flux control and the torque control of the induction motor are completely decoupled, the q-axis component rotor flux should be zero at the steady state. Both the ADRC and the PI control do not make the q-axis component rotor flux to be zero, but the steady-state error of the q-axis rotor flux of the ADRC is obviously less than that of the PI control. It means that the decoupling degree of the proposed scheme is better than that of PI control.

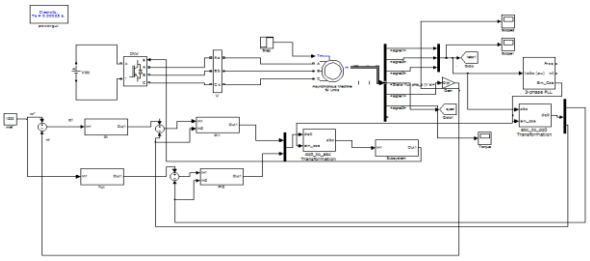

Fig 6.Simulation diagram by using PI controller

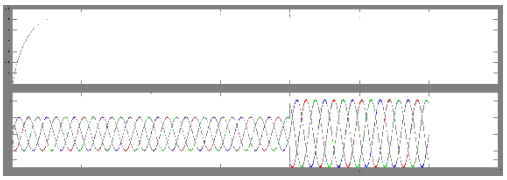

Speed and Current characteristics by using PI controller

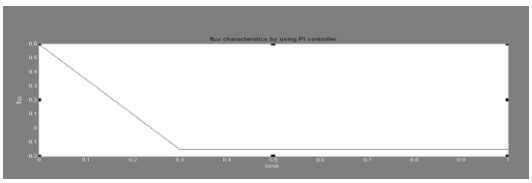

Flux characteristics by using PI controller

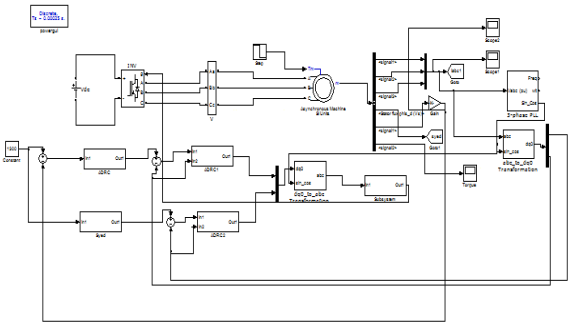

Simulation diagram by using higher order ADRC

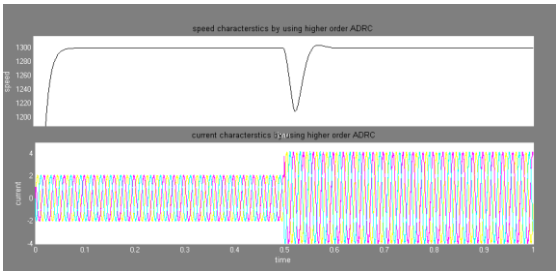

Speed and current characteristics by using higher order ADRC

IJIREEICE

ISSN (Online) 2321 – 2004
ISSN (Print) 2321 – 5526

International Journal of Innovative Research in
Electrical, Electronics, Instrumentation and Control Engineering

ISO 3297:2007 Certified

Vol. 4, Issue 9, September 2016

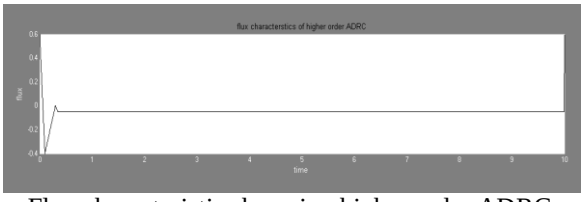

Flux characteristics by using higher order ADRC

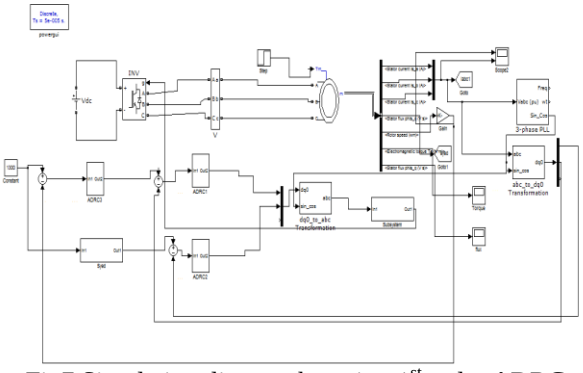

Fig7.Simulation diagram by using 1st order ADRC

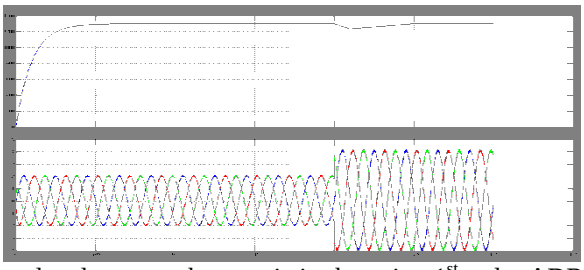

Speed and current characteristics by using 1st order ADRC

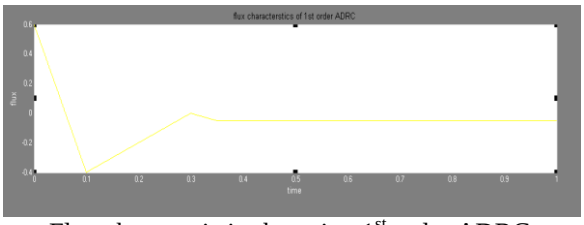

Flux characteristics by using 1st order ADRC

V. CONCLUSION

In this paper, the auto disturbance rejection controller (ADRC) has been applied to the induction motor control. The basis of ADRC is the extended state observer and nonlinear feedback control. The state estimation and compensation of the change of motor parameters and load variations are implemented by ESO and NLSEF. By using ESO, the complete decoupling of the induction motor is obtained. The generalized derivatives of given signals are achieved accurately. The major advantage of the proposed method is that the closed loop characteristics of the motor drive system do not depend on the exact mathematical model of the induction motor. Comparisons were made in detail between ADRC and conventional PI controller. It is concluded that the proposed control algorithm produces better dynamic performance than the PI controller and higher order ADRC. As verified with simulation results, the proposed ADRC control employing three first-order ADRCs has been presented in this paper for the robust control of induction motor drives fed by VSIs. Because the orders of the ADRCs are the lowest ones and the removal of the flux observer, the corresponding ADRC algorithms are simpler and have faster running speed compared with the existing ADRC(s) schemes. This is very important for real-time applications.

REFERENCES

[1] J. A. Santisteban and R. M. Stephan, "Vector control methods for induction machines: An overview," IEEE Trans. Educ., vol. 44, no. 2, pp. 170–175, May 2001.

[2] H. A. Toliyat, E. Levi, and M. Raina, "A review of RFO induction motor parameter estimation techniques," IEEE Trans. Energy Convers., vol. 18, no. 2, pp. 271–283, Jun. 2003.

[3] W. Gaolin, Y. Rongfeng, Y. Yong, C. Wei, and X. Dianguo, "Adaptive robust control for speed sensorless field-oriented controlled induction motor drives," (in Chinese), Trans. China Electrotech. Soc., vol. 25, no. 10, pp. 73–80, Oct. 2010.

[4] Z. Chunpeng, L. Fei, S.Wenchao, and C. Shousun, "Back-stepping design for robust controller of induction motors," (in Chinese), Control Decision, vol. 19, no. 3, pp. 267–271, Mar. 2004. 720 IEEE TRANSACTIONS ON INDUSTRY APPLICATIONS, VOL. 51, NO. 1, JANUARY/FEBRUARY 2015

[5] C.-Y. Huang, T.-C. Chen, and C.-L. Huang, "Robust control of induction motor with a neural-network load torque estimator and a neural-network identification," IEEE Trans. Ind. Electron., vol. 46, no. 5, pp. 990–998, Oct. 1999.

[6] T.-C. Chen and T.-T. Sheu, "Model reference neural network controller for induction motor speed control," IEEE Trans. Energy Convers., vol. 17, no. 2, pp. 157–163, Jun. 2002.

[7] J. Han, "From PID to active disturbance rejection control," IEEE Trans. Ind. Electron., vol. 56, no. 3, pp. 900–906, Mar. 2009.

[8] J. Han, "Auto-disturbances-rejection controller and its applications," (in Chinese), Control Decision, vol. 13, no. 1, pp. 19–23, 1998.

[9] J. Han, "Nonlinear design method for control systems design," in Proc. 14th Int. IFAC World Congr., Beijing, China, 1999, pp. 230–235.

[10] L. Shunli, Y. Xu, and Y. Di, "Active disturbance rejection control for high pointing accuracy and rotation speed," Automatica, vol. 45, no. 8, pp. 1854–1860, Sep. 2009.

[11] Y. Zhang, D. Li, and Y. Xue, "Active disturbance rejection control for circulating fluidized bed boiler," in Proc. 12th ICCAS, Jeju, Korea, Oct. 2012, pp. 1413–1418.

[12] Q. Zhong, Y. Zhang, J. Yang, and J. Wu, "Non-linear auto-disturbance rejection control of parallel active power filters," IET Control Theory Appl., vol. 3, no. 7, pp. 907–916, Jul. 2009.

[13] Z. Hui, L. Bin, and Y. You-jun, "The auto-disturbance rejection simulation and research of double-fed wind turbine," in Proc. ICMTMA, 3rd, Jan. 2011, pp. 712–715.

[14] H.-P. Ren, J. Zhang, Q. Li, and D. Liu, "Brushless DC motor speed control based on active disturbance rejection controller," (in Chinese), Elect. Drive, vol. 38, no. 4, pp. 46–50, 2008.

[15] H.-P. Ren and F. Zhu, "Optimal design of adaptive disturbance reject controller for brushless DC motor using immune clonal selection algorithms," (in Chinese), Elect. Mach. Control, vol. 14, no. 9, pp. 69–74, 2010.